Article

Effect of Chemical Pre-Treatment on the Catalytic Performance of Oil Palm EFB Fibre Supported Magnetic Acid Catalyst

Shamala Gowri Krishnan [1], Fei Ling Pua [2,3,*] and Zhang Fan [4]

[1]   College of Graduate Studies, Universiti Tenaga Nasional, Kajang 43000, Selangor, Malaysia;
       shamala.gowri@uniten.edu.my
[2]   Institute of Sustainable Energy (ISE), Universiti Tenaga Nasional, Kajang 43000, Selangor, Malaysia
[3]   Department of Mechanical Engineering, College of Engineering, Universiti Tenaga Nasional,
       Kajang 43000, Selangor, Malaysia
[4]   Biomass Group, Key Laboratory of Tropical Plant Resources and Sustainable Use, Xishuangbanna Tropical
       Botanical Garden, Chinese Academy of Sciences, 88 Xuefulu, Kunming 650223, China; zhangfan@xtbg.ac.cn
*   Correspondence: gracepua@uniten.edu.my

Abstract: The development of heterogenous catalysts using renewable materials has received wide attention. A heterogenous catalyst has been a preferred choice as it evades the disadvantages of homogeneous catalysts, nevertheless, heterogenous catalysts has limited activity and a longer separation process. The current study emphasises the preparation of a new magnetic catalyst using oil palm empty fruit bunch (EFB) fibre as a carbon-based support material. The effect of different alkaline pre-treatments over the methyl ester conversion rate were investigated. The catalyst preparation parameters were studied by using the single factor optimisation approach, including the fibre loading, impregnation time, calcination temperature, and calcination time. Their effects in the esterification of oleic acid were investigated in this study. The optimisation study shows that the Na_2CO_3-treated(T)-EFBC magnetic catalyst had the highest esterification rate of 93.5% with 7 g EFB fibre loading, a 2 h impregnation time and a calcination temperature of 500 °C for 2 h. The catalyst possessed a good acidity of 3.5 mmol/g with excellent magnetism properties. This study showed that the catalysts are magnetically separable and exhibited good stability with 82.1% after five cycles. The oil palm EFB supported magnetic acid catalyst indicates it as a potential option to the existing solid catalysts that is economical and environmentally friendly for the esterification process.

Keywords: biomass; catalyst; magnetic; oil palm; oleic acid; energy

1. Introduction

The impact of global warming and the steady depletion of non-renewable energy resources, such as fossil fuels, has led many researchers worldwide to intensively investigate a potential substitution for fossil fuels [1]. With the increased attention in identifying new resources, biodiesel, a mixture of fatty acid alkyl esters, is gaining much global interest due to it being non-toxic, renewable, sustainable and environmentally benign. Traditionally, homogeneous catalysts, such as sodium hydroxide (NaOH), potassium hydroxide (KOH) and sulphuric acid (H_2SO_4), were used for biodiesel production. Despite their effective catalytic activity to produce a high biodiesel yield, these catalysts, however, are noted to be non-environmentally friendly as they are unrecyclable [2,3]. Besides having no catalyst recyclability, contributing to equipment corrosion, there is the unavailability of the final product to recover the catalyst due to its solubility nature resulting in further purification processes, which leads to the production of large amounts of wastewater [4].

The development of a new heterogeneous catalyst for the catalytic process involves the identification of a potential catalyst that can address the difficulties of using a homogeneous catalyst in biodiesel production. Further, through a heterogeneous catalytic process, there is a high possibility of obtaining a catalyst that can be recycled with the catalytic functions

of the acidic sites on the surface and that does not cause any damage to the equipment [5]. Many metal oxides catalysts, such as mixed metal oxides, zeolites, graphene oxides, sulphated zirconia/titanium and ionic liquids, have been extensively used in the biodiesel production process as they have high stability and a reduced effect on the ecosystem [6]. Despite their good stability and eco-friendliness, the difficulty in the separation of catalysts from a large-scale reaction product is still unresolved.

Over the years, several researchers have focused on the use of biomass or carbon-based materials for solid catalyst synthesis. A study conducted by Tang and Niu on the preparation of carbon-based solid catalysts from bamboo for the esterification reaction reported that a high surface area of $1208 \text{ m}^2/\text{g}$ helped to achieve a high biodiesel yield of 97.3% [7]. The study showed that biomass-based catalysts are non-toxic, biodegradable and possess a high surface area for a higher yield, thus proving that it can be a potential replacement for the existing conventional catalyst. Additionally, another study on heterogeneous catalysts, graphene oxide and sulfonated biochar for lactic acid esterification reported that the highest yield of 35% was obtained after 420 min [8]. Although many solid catalysts have been investigated in the past, the technical difficulty in separating the solid catalysts from the product either by filtration or centrifugation remains as the main drawback, whereby more time is required, and the catalyst is lost during the recovery process [9]. In regard to this, several authors have claimed that the catalytic activity of sulphate metal oxide could be enhanced by their rapid separation from the products [10,11].

Recently, the use of a magnetic catalyst has gained much interest due to its easy separation from the product by using an external magnet. Feyzi and Norouzi worked on a novel magnetic $Ca/Fe_3O_4@SiO_2$ nano-catalyst for biodiesel production and further reported that the catalytic performance of this catalyst proved to exhibit a high biodiesel yield of 97% [12]. Besides, Gardy et al. also acquired excellent catalytic activity for the methyl oleate and biodiesel production over a magnetic core-shell catalyst, with the highest yield of 88% and 98.5%, respectively [13].

Agricultural waste is often referred to as lignocellulosic material consisting of lignin, cellulose and hemicellulose [14]. Due to its limited usability and only as a possible source of electricity and heat energy, the agricultural waste had low market value. However, agricultural biomass is naturally composed of carbons that can be utilised as recyclable carbon materials. As oil palm is one of Malaysia's mainly grown crops with vast production, enormous amounts of palm waste, such as oil palm fronds, trunks, empty fruit bunches, shells and kernels, have been generated [15,16]. The oil palm empty fruit bunch (EFB), which is of particular interest in this study, is produced as waste after the harvesting process, whereby the oil extraction is done and primarily used as a power source in palm oil mill incinerators [17]. Further, EFB, which is abundant within the lignocellulosic component, can be a potential source of sustainable biomass.

This study aims to synthesise a magnetic solid catalyst using raw EFB fibres and chemically treated fibres via a one-step impregnation and calcination method. The catalyst was then used in the catalytic esterification of oleic acid and the catalytic performance was evaluated through the optimisation of several parameters during the catalyst preparation process. The synthesised catalyst was characterised by morphological analysis, elemental analysis and an acid density test. Meanwhile, the esterified product from the catalysed reactions at the optimum condition was analysed using gas chromatography (GC) analysis.

2. Materials and Methods

2.1. Materials

Oil palm empty fruit bunch (EFB) fibres were collected from Sztech Engineering Sdn. Bhd. (Shah Alam, Selangor, Malaysia). Analytical reagents, including ferric sulphate ($Fe_3(SO_4)_2$), ferrous sulphate heptahydrate ($FeSO_4.7H_2O$), sodium bicarbonate (Na_2CO_3), potassium oxide (KOH), calcium hydroxide ($Ca(OH)_2$) and sodium hydroxide (NaOH) chemicals used for the catalyst preparation were purchased from Suria Pembekal Umum

Sdn. Bhd. (Kuala Lumpur, Malaysia). Industrial oleic acid with an acid value of 199 mg KOH/g (R&M, Petaling Jaya, Selangor, Malaysia) used in the esterification reaction.

2.2. EFB Fibre Chemical Pre-Treatment

The raw EFB fibres were ground and sieved to the size range of 125–150 μm. Next, the fibres were pre-treated with 0.1 M NaOH solution, and a solid-to-liquid ratio of 50 g/L was employed. The oven-dried EFB fibres were pre-treated by stirring in the NaOH solution for 1 h with agitation at a speed of 350 rpm at room temperature. The fibres were immersed in the alkali solution for 30 min after the process. The fibres were then washed repeatedly with distilled water to remove the excess chemical until a neutral pH (~pH 7) was achieved. The washed fibres were then poured onto an aluminium tray and oven-dried for 24 h at 105 °C. The same method was used to study the effect of chemical modification using various alkalines, including KOH, $Ca(OH)_2$ and Na_2CO_3, with the same concentration (0.1 M). All treated fibres were stored for further use.

2.3. Synthesis of the Magnetic Solid Catalyst

The magnetic solid catalyst was synthesised via the one-step impregnation method. Firstly, the method was conducted by mixing the treated EFB fibres with a 0.01 M $FeSO_4.7H_2O$ and 0.02 M $Fe_3(SO_4)_2$ solution with continuous stirring at 60 °C for 2 h. A solid-to-liquid ratio of 1:10 was employed. The solid was then oven-dried overnight at 80 °C. Following that, the oven-dried samples were calcined using a vacuum furnace. Figure 1 shows the summary of the magnetic catalyst synthesis. The EFB magnetic catalyst was prepared using fibres treated differently with NaOH, KOH, $Ca(OH)_2$ and Na_2CO_3, denoted as NaOH-T-EFBC, KOH-T-EFBC, $Ca(OH)_2$-T-EFBC and Na_2CO_3-T-EFBC, respectively.
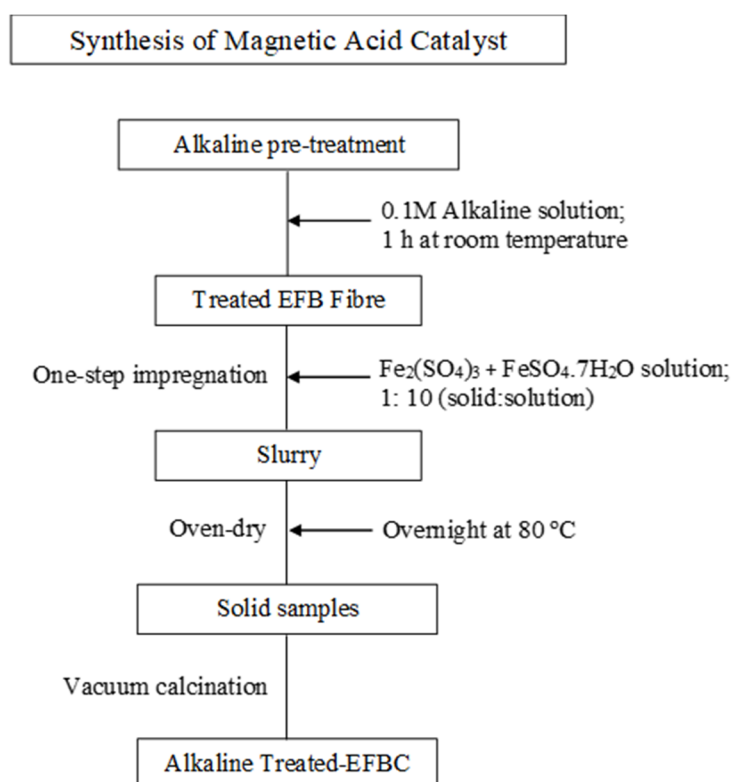

Figure 1. The summary of the magnetic acid catalyst preparation.

Later, the catalyst synthesis parameter conditions were optimised in terms of fibre loading, reaction time, calcination temperature and calcination time via the single factor

optimisation method. Table 1 shows the parameters and ranges for the optimisation of the esterification reaction of oleic acid.

Table 1. The parameters and ranges for the optimisation study.

Factors	Unit	1	2	3	4	5
EFB fibre loading	g	1	3	5	7	9
Reaction time	h	1	2	3	4	5
Calcination temperature	°C	300	400	500	600	700
Calcination time	h	1	2	3	4	5

2.4. Characterisation of the Fibre and Catalyst

The lignin content analysis was conducted using the acid detergent lignin (ADL) method at MARDILab, Technical Services & Technology Commercialization Centre (Serdang, Selangor, Malaysia). With regards to the characterisation, the morphology and elemental composition of the samples were analysed by using a scanning electron microscopy (SEM) equipped with energy-dispersive X-ray spectroscopy (EDS) (JSM-6010PLUS/LV, Universiti Tenaga Nasional, Kajang, Malaysia). The acidity of the solid acid catalyst was determined by using the acid–base titration method. The method involved titrating with sodium hydroxide solution (0.1 M NaOH), with phenolphthalein as an indicator. The data was recorded, and the acid density was calculated using Equation (1):

$$\text{Acidic} = \frac{[\text{OH}] \times \text{VOH}}{\text{m}} \tag{1}$$

[OH] = concentration of NaOH used, VOH = volume of NaOH required and m = mass of catalyst.

2.5. Catalytic Performance

In total, 7 wt% of solid catalyst was mixed with 10:1 methanol and pre-heated oleic acid in a three-neck flat-bottom flask at 60 °C for 2 h at 350 rpm. The solid magnetic acid catalyst was separated by an external magnet, washed with ethanol and oven-dried at 80 °C for further use. The collected liquid was then heated at 70 °C to evaporate the excess methanol.

Next, the methyl ester conversion was examined via the base titration method using KOH. The data was collected, and the acid value of the esterified sample and oleic acid was calculated based on the ASTM D664 standard method (Equation (2)) [18], while the esterification conversion rate was calculated using Equation (3) [19]:

$$\text{Acid value} = \frac{([\text{OH}] \times \text{V} \times \text{MM})}{\text{m}} \tag{2}$$

$$\text{Conversion rate (\%)} = \left(\frac{(\text{AV}_\text{i} - \text{AV}_\text{o})}{\text{AV}_\text{i}} \times 100 \right) \tag{3}$$

V = volume of KOH titrated in mL, MM = molecular mass of KOH, [OH] = concentration of KOH, m = mass of catalyst, AV_i = initial acid value and AV_o = acid value of methyl oleate.

3. Results and Discussion

3.1. Effect of Various Chemical Pre-Treatments on the Esterification Reaction

NaOH, KOH, $Ca(OH)_2$ and Na_2CO_3 are the essential alkalis used in the alkaline pretreatment to investigate their efficiency in the delignification process. The pre-treatment process generally signifies the removal of lignin from lignocellulose material. The removal of complex lignin attributes to the loosening of the crystalline structure of cellulose and enhances the porosity of the biomass for catalyst preparation [20]. After alkaline pre-treatment, the lignin content changed significantly and altered the surface texture of

the fibres. Lignin content is considered an important component influenced by alkaline pre-treatment because lignin forms a three-dimensional network between cellulose and hemicellulose [21]. The lignin content resulted in a range of 13.7–15.1% by using for different alkalis at a standardised concentration (Figure 2). The results showed the percentage of lignin content reduced after alkaline treatment compared to the untreated EFB fibres, with 16.5%, and this is similar to that reported by Ariffin et al. [22]. The effect of various alkaline pre-treatments resulted 14.5%, 13.7%, 14.1% and 15.1% using NaOH, KOH, $Ca(OH)_2$ and Na_2CO_3, respectively. Alkaline pre-treatment contributes to the chemically modified structure of lignocellulosic EFB, breaking up the crystalline structure and increasing the accessible surface area of EFB for a better interaction with metal sulphates in catalyst preparation [23].
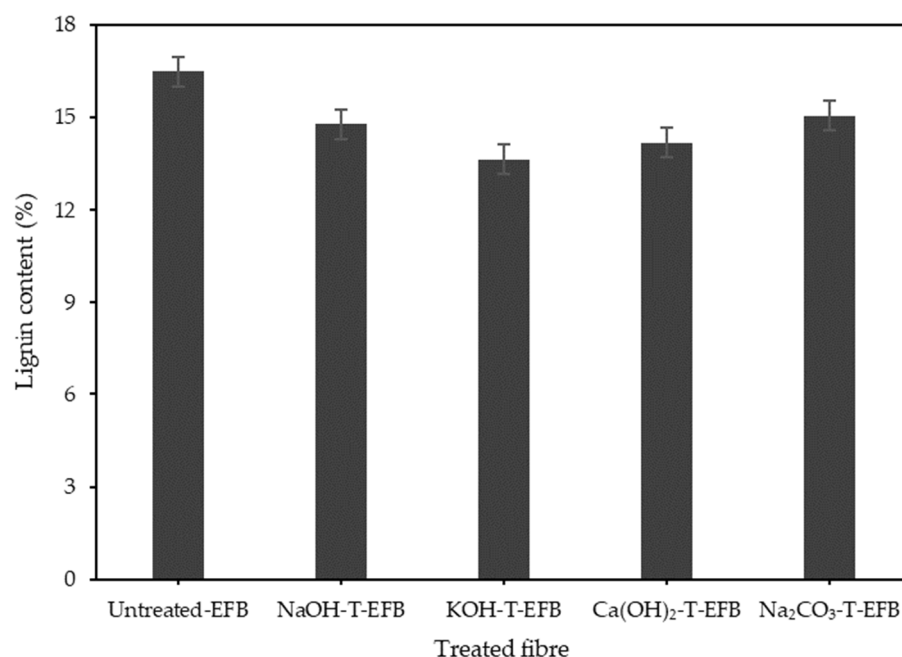

Figure 2. Effect of chemical pre-treatment on the EFB fibre delignification.

The trends in the catalysts' acidity and conversion rate over different alkaline pre-treatments and untreated-EFB are shown in Figure 3. After alkaline pre-treatment, the treated EFB fibres were used in the synthesis of magnetic solid catalysts. Five grams of treated EFB fibres were added into the chemical solution (1:10) and stirred for 2 h at 60 °C. The dried sample was calcined at 500 °C for 3 h in a vacuum furnace. The results indicated that the highest catalyst acidity was reported for catalysts treated by $Ca(OH)_2$ and Na_2CO_3, with 3.5 mmol/g, compared to the catalysts treated by NaOH and KOH, which were 3.3 mmol/g and 2.5 mmol/g, respectively. Moreover, both $Ca(OH)_2$-T-EFBC and Na_2CO_3-T-EFBC catalysts observed a higher conversion rate of 85.1% and 87.8%, respectively, compared with the catalysts treated by NaOH, KOH and untreated-EFB, which had 80.6%, 74.5% and 79.03, respectively. The highest acidity and conversion rate wsd obtained in EFB treated with Na_2CO_3 (Na_2CO_3-T-EFB), showing that Na_2CO_3 pre-treatment has a significant effect on the conversion rate. The dissociation of Na_2CO_3 in water produces carbonic acid, and sodium hydroxide that has the potential to disrupt the structure and remove silica on the EFB fibre surface [24]. Although the lignin content for Na_2CO_3-T-EFB is higher compared to other alkaline treatments, the esterification rate was exhibited to be higher using the derived catalyst. This could be due to the existence of hydrophilic and hydrophobic groups, such as hydroxyl groups and polycyclic aromatic carbons, in the carbonaceous catalyst [25]. The reactants can easily be absorbed onto the solid catalyst surface to contact with the active sites. The active sites of sulfonic acid ($-SO_3H$) and iron

oxide (Fe-O) are known as Bronsted acid and Lewis acid, respectively, which contribute to a higher conversion rate [26].
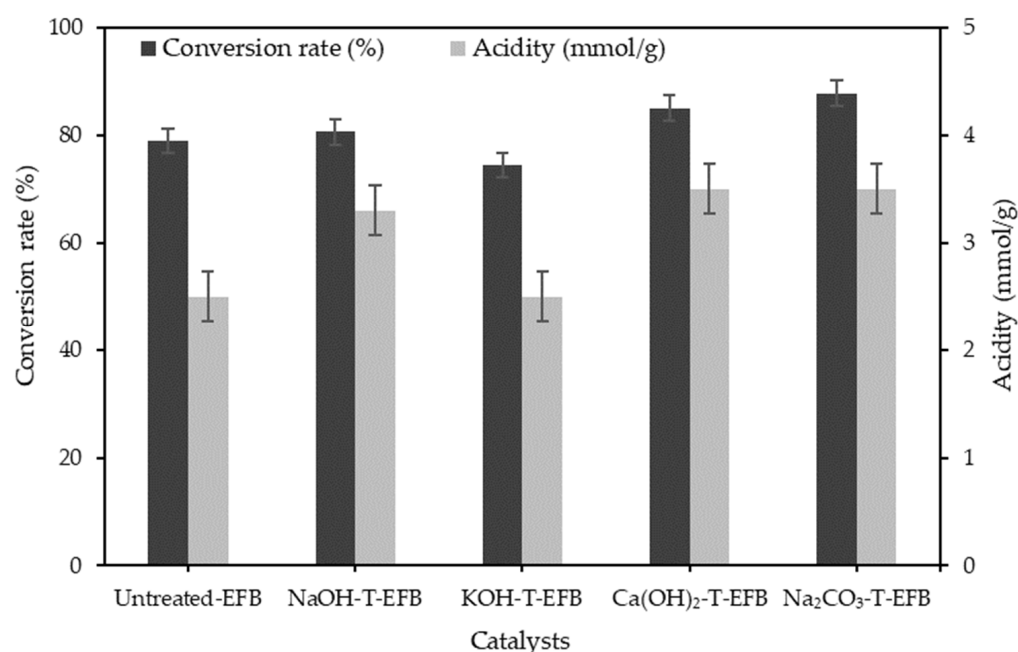

Figure 3. The relationship between chemically treated EFB fibre-derived magnetic catalysts with the acidity and esterification rate.

3.2. Single Factor Optimisation

As the Na_2CO_3-T-EFBC magnetic catalyst recorded the highest conversion rate, the Na_2CO_3 treated EFB fibres were utilised to investigate the effect of catalyst synthesis parameters, such as EFB treated fibre loading, impregnation time, calcination temperature and calcination time, on conversion rate and catalyst acidity (Figure 4a–d). The effect of EFB fibre loading on the conversion rate is demonstrated in Figure 4a. As aforementioned, the catalyst was synthesised with different ranges of EFB fibre loading by weight (1, 3, 5, 7 and 9 g). As shown in Figure 4a, the findings indicated an increase in the conversion rate from 78.32% to 91.18% as the EFB fibre loading increased from 1 g to 7 g. The increment of the esterification rate was observed to increase with the incline in the catalyst acidity from 1.7 mmol/g to 2.2 mmol/g. The findings are supported by a previous study by Jing et al., which stated that the concentration of support material or precursor is one of the key factors that affects the preparation of the catalyst by the impregnation method [27]. Further, as biomass consists of a more complex polymer structure, which is made up of functional oxygenated molecules, namely, carboxyl (-COOH) and hydroxyl (-OH) [28], the addition of carbon material enhanced the existence of weak Bronsted acid sites in the catalyst surface besides the presence of sulfonic acid (-SO_3H) sites [29]. Thus, the 7 g EFB fibre loading significantly increased the esterification rate with the highest acidity of 2.2 mmol/g, and the esterification reaction was favoured by the high acidity of the catalyst. However, a further increment in the amount of EFB fibre loading (9 g) was insignificant in the esterification reaction of oleic acid. This could be attributed to the limited active sites and the lack of strong acid sites for the catalytic reaction, which resulted in a slight reduction in the conversion rate to 90.81% with an acidity of 2.1 mmol/g.

In order to investigate the effect of the impregnation time in the conversion rate, different reaction times of 1, 2, 3, 4 and 5 h were executed. Figure 4b illustrates that the conversion rate increases with the increase in the impregnation time. It was observed that as the impregnation time increased from 1 to 2 h, the conversion rate was observed as 88.02% and 91.18%, respectively. During the impregnation process, the interaction through absorption between the pores of the support material with the bulk solution used requires

a certain time to occur [30]. However, no significant effect was detected in the oleic acid conversion after 2 h of impregnation time, which was similar to the decline in the acidity of the catalyst after 3 to 5 h of the impregnation time. The low acidity contributed to the decrease in the conversion rate from 89.32% to 79.87% after 5 h. A previous study reported that the impregnation time highly depended on the support size, loading amount and the temperature [31]. Based on the observation, at 2 h of impregnation time, the ferric sulphate particles may be mostly adsorbed on the surface of the treated EFB fibres. Hence, at further impregnation times, the particles have limited sites available for absorption, which reasons the lower conversion rate of oleic acid after 2 h of impregnation time. Therefore, to achieve a high conversion rate and the efficient formation of active sites, an appropriate impregnation time is required; thus, the 2 h reaction time was found to be favourable for high catalytic performance [32].
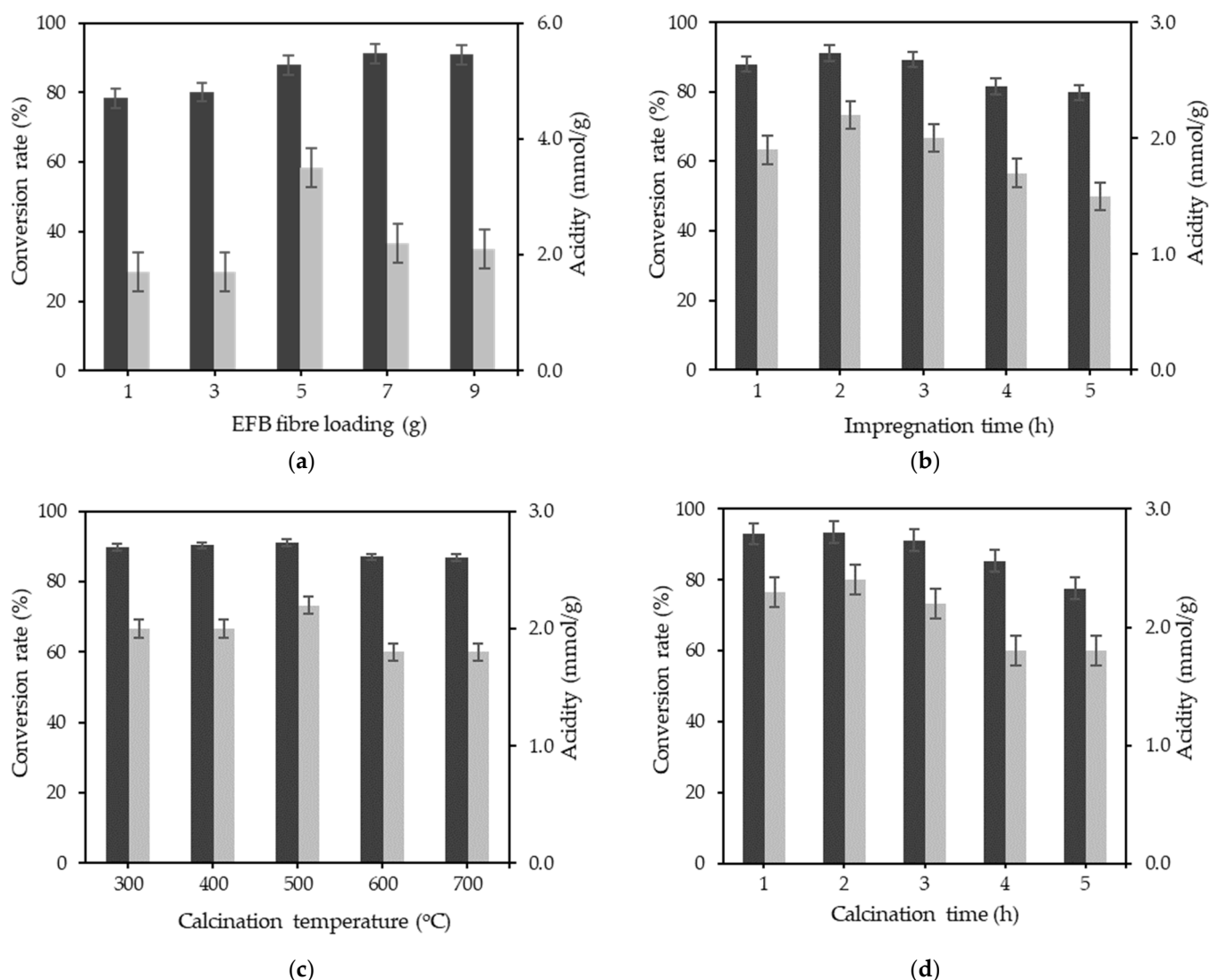

Figure 4. Optimisation studies for catalyst preparation. (**a**) Effect of EFB fibre loading (2 h impregnation time and calcination at 600 °C for 3 h). (**b**) Effect of impregnation time (EFB fibre loading 7 g and calcination at 600 °C for 3 h). (**c**) Effect of calcination temperature (EFB fibre loading 7 g, 2 h impregnation time and calcination for 3 h). (**d**) Effect of calcination time (EFB fibre loading 7 g, 2 h impregnation time and calcination at 500 °C).

Calcination temperature is an essential factor for a catalyst because of its effect on the structural and catalytic properties [33]. The effect of calcination temperature on oleic acid conversion was studied, and the results are shown in Figure 4c. The magnetic catalyst was

calcined using a vacuum furnace at various calcination temperatures of 300, 400, 500, 600 and 700 °C. The findings indicated that the conversion rate gradually increases from 300 °C to 500 °C with values of 89.95% and 91.18%, respectively. This shows that calcination temperature has a significant effect on the catalytic activity as the temperature improves the formation of particles on the catalyst surface [34]. However, a gradual decrease in the conversion rate was noted at a higher temperature, which indicates that calcination at a higher temperature would contribute to sintering of particles on the surface of the support material, thus, resulting in a decrease in surface area, which eventually affects the catalytic activity [35]. Previous studies have also stated that a suitable calcination temperature was required for an effective esterification reaction because both low and high calcination temperatures were not beneficial for the conversion of oleic acid [36,37]. Hence, the suggested 500 °C was determined as an optimum temperature for the calcination process of the catalyst.

The effect of the calcination time on the esterification rate was also investigated to determine the optimum catalyst preparation parameters. The catalyst was calcined for a range of calcination times (1, 2, 3, 4 and 5 h) at a fixed temperature of 500 °C. Figure 4d presents the summary of the findings. It was found that calcination for 2 h produced an active catalyst with the maximum conversion rate of 93.46% and an acidity of 2.4 mmol/g. The high rate was attributed to the sufficient time for the formation of active components, which helps to increase the conversion rate [38]. Furthermore, the results show that the increment in calcination time was not favourable for esterification as the conversion rate gradually decreased to 77.62% after 5 h of calcination. A reason for this could be the particle sintering or agglomeration on the catalyst surface, which resulted in weak catalytic activity after a longer calcination duration [39]. Besides, a longer calcination time could deactivate the catalyst's acidic sites [40]. Thus, an optimum calcination time of 2 h was essential to synthesise an EFB supported magnetic acid catalyst. The optimum conditions for catalyst preparation are: 7 g EFB fibre loading, 2 h impregnation time and a calcination temperature of 500 °C for 2 h.

3.3. Morphology and Elemental Analysis

Additionally, scanning electron microscopy (SEM) was used to evaluate the morphology of the raw EFB fibres, treated EFB fibres and the magnetic acid catalyst. Figure 5 depicts the SEM observations of the effect of alkaline treatment on the EFB fibre surface. Figure 5a indicates the presence of white granules, known as silica bodies, and impurities on the surface of raw EFB fibres. However, these impurities and silica bodies were removed from the EFB surface after the alkaline treatment using sodium carbonate, Na_2CO_3, as illustrated in Figure 5b. Rosli et al. reported that the silica bodies are known as phytoliths, which are found on the fibre surface and could lead to poor adsorption of particles on the fibre surface [41]. After the silica bodies were removed using an alkaline treatment, a rough surface and the appearance of tiny pores were noticed. Meanwhile, the SEM image of a treated fibre impregnated with sulphated and iron oxide particles is presented in Figure 5c. It showed that the catalyst had a rough surface, with the particles embedded on the EFB surface after calcination at 500 °C for 2 h.

In addition, Table 2 presents the energy-dispersive spectrometry (EDS) results of treated EFB fibres and the Na_2CO_3-T-EFB magnetic catalyst. The treated fibres, which consist of pure carbon and oxygen, indicates that alkaline pre-treatment improves the EFB fibre surface. Meanwhile, the EDS result of the impregnated catalyst shows the existence of carbon (C), iron (Fe), oxygen (O) and sulphur (S) groups embedded on the surface of treated EFB fibres with 37.88 wt%, 21.82 wt%, 34.78 wt% and 5.52 wt%, respectively. Hence, the oxygen and sulphur content could indicate the existence of the sulfonic group (-SO_3H) in the catalyst [19]. Besides, the composition of iron and oxygen indicate that the catalyst is comprised of Fe-O particles, which further induces its magnetic properties.
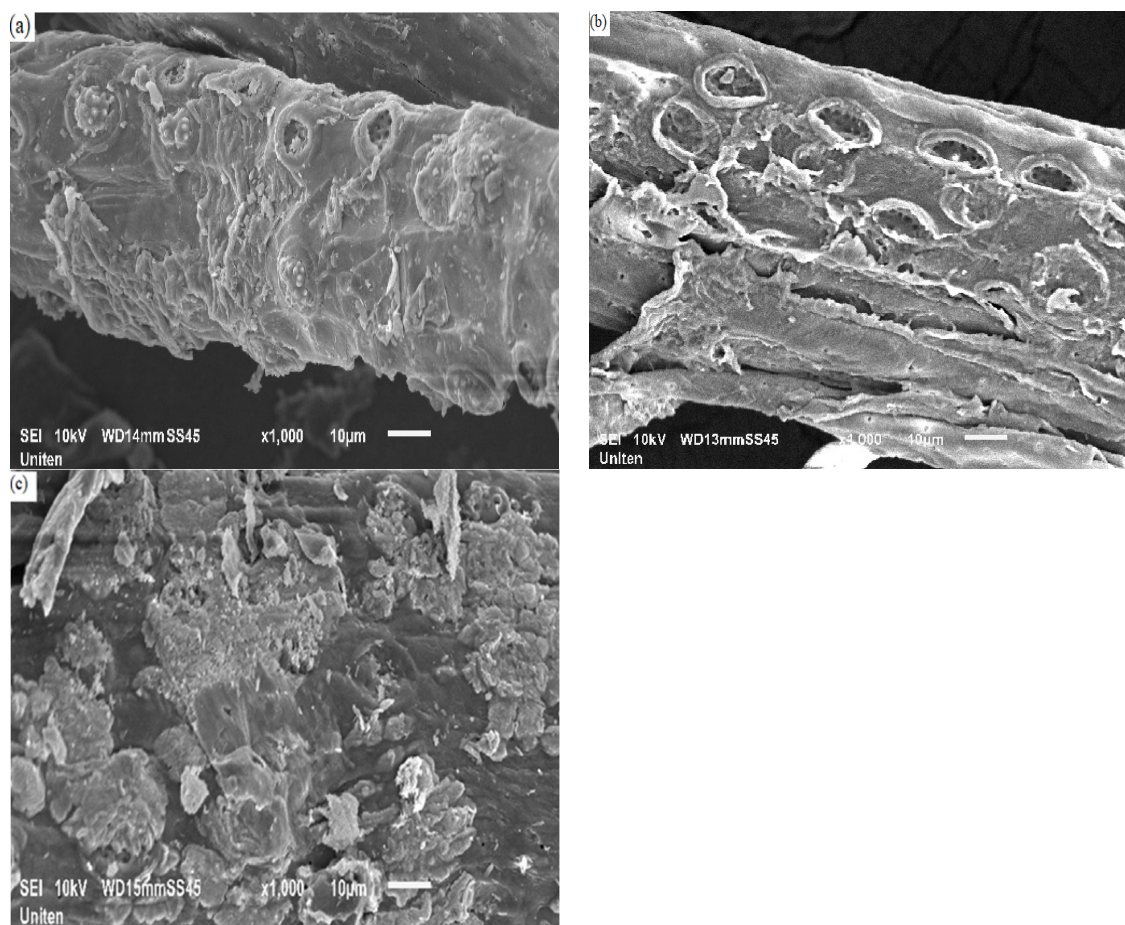
Figure 5. SEM images of (**a**) raw EFB fibre, (**b**) Na$_2$CO$_3$-T-EFB, and (**c**) Na$_2$CO$_3$-T-EFB derived magnetic acid catalyst.

Table 2. Elemental composition of treated EFB fibres and the EFB supported magnetic acid.

Samples	Elemental Composition (wt%)			
	Carbon (C)	**Oxygen (O)**	**Iron (Fe)**	**Sulphur (S)**
Treated EFB fibres	57.76	42.24	n.d [a]	n.d [a]
Na$_2$CO$_3$-T-EFB magnetic catalyst	37.88	34.78	21.82	5.52

[a] n.d = not determined.

3.4. Catalyst Reusability

The performance of the Na$_2$CO$_3$-T-EFBC magnetic catalyst was tested using the esterification reaction of oleic acid at 60 °C for 2 h, which obtained a conversion rate of 93.5% (Figure 6). After the reaction, the used catalyst was collected by using an external magnet and was washed and dried to be used in the next cycle of esterification. It was observed that the conversion rate decreased in the second cycle to 89.5%, which was possibly due to the leaching of active sites from the catalyst during the reaction. However, the conversion rate slightly dropped to 86.3% and the catalytic activity was further retained between 82.9 and 82.1% after the fourth and fifth cycles. It was noticed that the catalyst performance remains stationary after the fifth cycle. The stability of conversion rate over Na$_2$CO$_3$-T-EFBC could be associated to the higher acidity after the fifth cycle of 2.8 mmol/g.
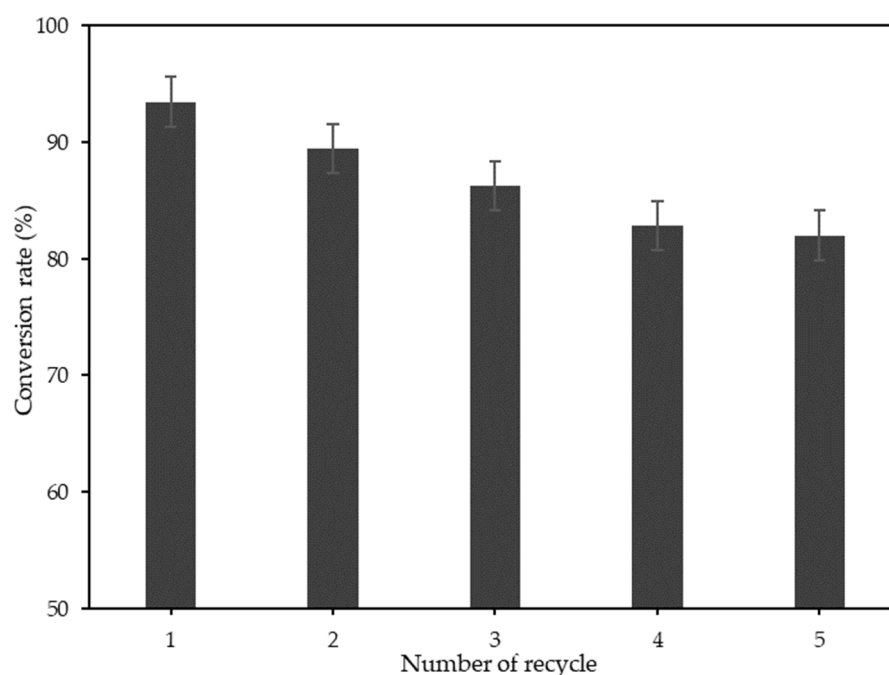
Figure 6. Reusability of the Na_2CO_3-T-EFB derived magnetic acid catalyst.

3.5. Comparison of Surface Acidity on the Catalytic Activity of Biomass Derived Solid Catalysts

The surface acidity over esterification performance of the biomass-based solid acid catalysts prepared in this study was compared with other studies in Table 3. It was observed that the Na_2CO_3-T-EFBC magnetic catalyst has a comparable or higher conversion rate at a shorter time of 2 h under a lower reaction temperature of 60 °C, which was attributed to the strong acidity on the catalyst surface. Most importantly, the magnetic catalyst prepared in this study had showed good stability compared to those in the studies reported. This proves that the Na_2CO_3-T-EFBC magnetic catalyst was exhibited as a practical catalyst for acid catalysed reactions.

Table 3. Comparison of the surface acidity over esterification performance of carbon-based solid acid catalysts prepared in this work with other studies.

Catalysts	Surface Acidity			Esterification Performance			Refs.
	By S Content (mmol SO_3H/g) [a]	By Base Titration (mmol/g)	By NH_3-TPD (mmol/g)	Conditions [b]	Conversion (%)	Reusability	
Spent coffee grounds-derived solid acid catalyst	3.36	4.22	-	CL of 10 wt%, MeOH:OA of 10:1, 80 °C/7 h	>90.0	~70% after 4 cycles	[42]
Cacao shell-derived solid acid catalyst	1.48	4.56	-	CL of 0.05 wt%, MeOH:OA of 7:1, 42 °C/4 h	78.0	48.0% after 3 cycles	[43]
EFB derived MBC02-SO_3H	-	-	0.28	CL of 5 wt%, MeOH:OA of 8:1, 150 °C/1.5 h	81.0	Not reported	[44]
Bamboo derived solid acid catalyst (S150-4)	0.82	-	-	CL of 10 wt%, MeOH:OA of 8:1, 65 °C/8 h	98.0	79.2% after 4 cycles	[45]
Dealkaline lignin derived E−260-20-SO_3H (Supercritical ethanol)	1.41	5.05	-	CL of 5 wt%, MeOH:OA of 12:1, 80 °C/7 h	95.4	≥81.9% after 5 cycles	[46]
Dealkaline lignin derived E-P400−2-SO_3H (Subcritical ethanol)	1.06	5.35	-	CL of 5 wt%, MeOH:OA of 15:1, 80 °C/5 h	95.5	≥84.6% after 3 cycles	
Na_2CO_3-T-EFBC magnetic catalyst	1.72	3.50	-	CL of 7 wt%, MeOH:OA of 10:1, 60 °C/2 h	93.5	82.1% after 5 cycles	This study

[a] Surface acidity by S content (mmol SO_3H/g) was calculated using the following formula: Surface acidity (mmol SO_3H/g) = (S content in catalyst/100) × 1000/32.07. [b] CL = catalyst loading, MeOH = methanol, OA = oleic acid.

3.6. Reaction Mechanism Using Na_2CO_3-T-EFBC

The possible reaction mechanism of the catalytic esterification of oleic acid with methanol using Na_2CO_3-T-EFBC is able to be described in several steps and is presented

in Figure 7. Meanwhile, -SO$_3$H groups derived from the magnetic acid catalyst catalyse the esterification reaction. Three-oxygen molecules accept electrons from sulphur to form electron-withdrawing (-SO$_3$H, sulfonic acid) groups, which act as the Bronsted acid active sites [47]. The catalytic mechanism involves several steps: (1) The strong H$^+$ proton of the catalyst attacks the oxygen in the carboxyl group of oleic acid during the reaction, (2) the alcohol molecule reacts with the activated carboxyl carbon through nucleophilic substitution, (3) the intramolecular dehydration and hydrogen ion desorption lead to the formation of water molecules, and lastly, (4) the formation of methyl esters. In addition, the Lewis acid nature of iron oxide (Fe-O) particles also serve as active sites and contribute to the catalytic activity.
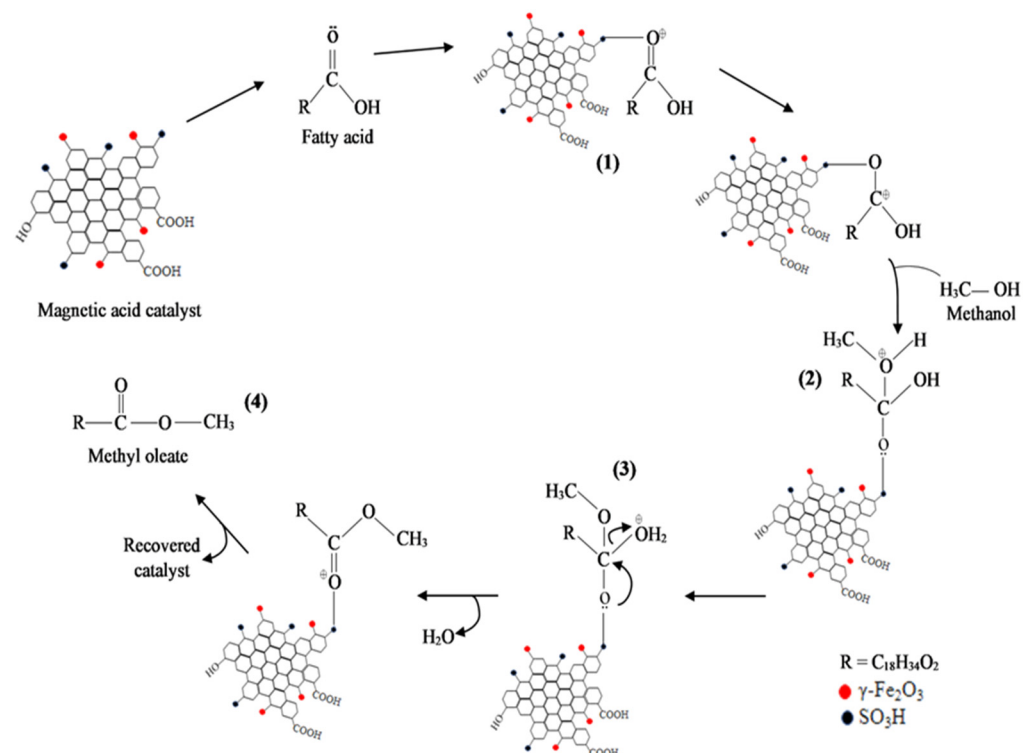
Figure 7. Proposed 4-step ((1)–(4)) reaction mechanism of the esterification of oleic acid using the Na$_2$CO$_3$-T-EFBC catalyst.

4. Conclusions

EFB fibres were utilised to produce efficient biomass-supported magnetic acid catalysts. The EFB fibre-supported magnetic acid catalyst was successfully synthesised and the performance of the catalyst was evaluated via the esterification of oleic acid. The effect of chemical pre-treatments on the catalytic performance and acidity were investigated, and the Na$_2$CO$_3$-T-EFBC magnetic catalyst showed a noticeable effect with a high conversion rate of 87.8%. Further, under the optimal catalyst preparation conditions of 7 g EFB fibres loading at 2 h impregnation time and 2 h of calcination at 500 °C, a high conversion rate of 93.46% was reported. The EFB fibre-supported magnetic catalyst revealed good properties with a high acidic value, indicating the existence of the sulfonic group, which interacts with methanol and oleic acid for the esterification reaction. Besides, the catalyst had strong magnetism, and it was recovered using an external magnet. The catalyst reusability showed good stability with 82.1% after five cycles. In conclusion, the EFB magnetic solid catalyst had good properties, such as strong magnetism and high acidity, with good catalytic performance. The findings in this study provide a potential substitution to be used as a green heterogeneous catalyst in the biodiesel industry. Thus, this assures the prominent usage of oil palm waste in wide applications and minimises waste.

References

1. Rath, B.N.; Akram, V.; Bal, D.P.; Mahalik, M.K. Do Fossil Fuel and Renewable Energy Consumption Affect Total Factor Productivity Growth? Evidence from Cross-Country Data with Policy Insights. *Energy Policy* **2019**, *127*, 186–199. [CrossRef]
2. Gebremariam, S.N.; Marchetti, J.M. Economics of Biodiesel Production: Review. *Energy Convers. Manag.* **2018**, *168*, 74–84. [CrossRef]
3. Faruque, M.O.; Razzak, S.A.; Hossain, M.M. Application of Heterogeneous Catalysts for Biodiesel Production from Microalgal Oil—A Review. *Catalysts* **2020**, *10*, 1025. [CrossRef]
4. Hsiao, M.C.; Kuo, J.Y.; Hsieh, S.A.; Hsieh, P.H.; Hou, S.S. Optimized Conversion of Waste Cooking Oil to Biodiesel Using Modified Calcium Oxide as Catalyst via a Microwave Heating System. *Fuel* **2020**, *266*, 117114. [CrossRef]
5. Ullah, F.; Dong, L.; Bano, A.; Peng, Q.; Huang, J. Current Advances in Catalysis toward Sustainable Biodiesel Production. *J. Energy Inst.* **2016**, *89*, 282–292. [CrossRef]
6. Chen, M.N.; Mo, L.P.; Cui, Z.S.; Zhang, Z.H. Magnetic Nanocatalysts: Synthesis and Application in Multicomponent Reactions. *Curr. Opin. Green Sustain. Chem.* **2019**, *15*, 27–37. [CrossRef]
7. Tang, X.; Niu, S. Preparation of Carbon-Based Solid Acid with Large Surface Area to Catalyze Esterification for Biodiesel Production. *J. Ind. Eng. Chem.* **2019**, *69*, 187–195. [CrossRef]
8. Vu, T.H.T.; Nguyen, M.H.; Nguyen, M.D. Synthesis of Acidic Heterogeneous Catalysts with High Stability Based on Graphene Oxide/Activated Carbon Composites for the Esterification of Lactic Acid. *J. Chem.* **2019**, *7815697*, 1–7. [CrossRef]
9. Gardy, J.; Osatiashtiani, A.; Céspedes, O.; Hassanpour, A.; Lai, X.; Lee, A.F.; Wilson, K.; Rehan, M. A Magnetically Separable SO_4/Fe-Al-TiO_2 Solid Acid Catalyst for Biodiesel Production from Waste Cooking Oil. *Appl. Catal. B* **2018**, *234*, 268–278. [CrossRef]
10. Kristiani, A.; Sembiring, K.C.; Aulia, F.; Abimanyu, H. Sulfated Zirconia Catalyst for Hydrolysis of Palm Oil Lignocellulosic Wastes. *Energy Procedia* **2015**, *65*, 8–13. [CrossRef]
11. Iwanow, M.; Gärtner, T.; Sieber, V.; König, B. Activated Carbon as Catalyst Support: Precursors, Preparation, Modification and Characterization. *Beilstein J. Org. Chem.* **2020**, *16*, 1188–1202. [CrossRef]
12. Feyzi, M.; Norouzi, L. Preparation and Kinetic Study of Magnetic Ca/Fe_3O_4@SiO_2 Nanocatalysts for Biodiesel Production. *Renew Energy* **2016**, *94*, 579–586. [CrossRef]
13. Gardy, J.; Nourafkan, E.; Osatiashtiani, A.; Lee, A.F.; Wilson, K.; Hassanpour, A.; Lai, X. A Core-Shell SO_4/Mg-Al-Fe_3O_4 Catalyst for Biodiesel Production. *Appl. Catal. B* **2019**, *259*, 118093. [CrossRef]
14. Loh, S.K. The Potential of the Malaysian Oil Palm Biomass as a Renewable Energy Source. *Energy Convers. Manag.* **2017**, *141*, 285–298. [CrossRef]
15. Thushari, I.; Babel, S. Sustainable Utilization of Waste Palm Oil and Sulfonated Carbon Catalyst Derived from Coconut Meal Residue for Biodiesel Production. *Bioresour. Technol.* **2018**, *248*, 199–203. [CrossRef]
16. Jafri, N.H.S.; Jimat, D.N.; Azmin, N.F.M.; Sulaiman, S.; Nor, Y.A. The Potential of Biomass Waste in Malaysian Palm Oil Industry: A Case Study of Boustead Plantation Berhad. *IOP Conf. Ser. Mater. Sci. Eng.* **2021**, *1192*, 12028. [CrossRef]
17. Dolah, R.; Karnik, R.; Hamdan, H. A Comprehensive Review on Biofuels from Oil Palm Empty Bunch (Efb): Current Status, Potential, Barriers and Way Forward. *Sustainability* **2021**, *13*, 10210. [CrossRef]
18. Zhang, Q.; Wu, J.; Ma, P.; Cai, J.; Zhang, Y. Acid Value Determination and Pre-Esterification of Crude Euphorbia Lathyris L. Oil. *World J. Eng. Technol.* **2015**, *3*, 70–75. [CrossRef]

19. Zhou, Y.; Niu, S.; Li, J. Activity of the Carbon-Based Heterogeneous Acid Catalyst Derived from Bamboo in Esterification of Oleic Acid with Ethanol. *Energy Convers. Manag.* **2016**, *114*, 188–196. [CrossRef]

20. Az-Zahraa, B.; Zakaria, S.; Daud, M.F.B.; Jaafar, S.N.S. Removal of Oil Palm Trunk Lignin in Ammonium Hydroxide Pretreatment. *AIP Conf. Proc.* **2018**, *1940*, 20017. [CrossRef]

21. Li, Y.; Li, F.; Yang, Y.; Ge, B.; Meng, F. Research and Application Progress of Lignin-Based Composite Membrane. *J. Polym. Eng.* **2021**, *41*, 245–258. [CrossRef]

22. Ariffin, H.; Hassan, M.; Umi Kalsom, M.; Abdullah, N.; Shirai, Y. Effect of Physical, Chemical and Thermal Pretreatments on the Enzymatic Hydrolysis of Oil Palm Empty Fruit Bunch (OPEFB) (Kesan Prarawatan Fizikal, Kimia Dan Termal Terhadap Hidrolisis Enzimitik Tandan Kosong Kelapa Sawit). *J. Trop. Agric. Food Sci.* **2008**, *36*, 259–268.

23. Ismail, S.; Saharuddin, M.Q.; Zahari, M.S.M. Upgraded Seawater-Alkaline Pre-Treatment of Lignocellulosic Biomass for Bio-Methane Production. *Energy Procedia* **2017**, *138*, 372–379. [CrossRef]

24. Chin, S.X.; Chia, C.H.; Zakaria, S.; Ahmad, S.H.; Tasirin, S.M. Combination of Gamma Irradiation and Sodium Carbonate Pretreatment on Oil Palm Empty Fruit Bunch (EFB) for High Acidic Hydrolysis Yield. *Sains Malays.* **2017**, *46*, 167–173. [CrossRef]

25. Guo, F.; Xiu, Z.L.; Liang, Z.X. Synthesis of Biodiesel from Acidified Soybean Soapstock Using a Lignin-Derived Carbonaceous Catalyst. *Appl. Energy* **2012**, *98*, 47–52. [CrossRef]

26. Wang, Y.T.; Yang, X.X.; Xu, J.; Wang, H.L.; Wang, Z.B.; Zhang, L.; Wang, S.L.; Liang, J.L. Biodiesel Production from Esterification of Oleic Acid by a Sulfonated Magnetic Solid Acid Catalyst. *Renew Energy* **2019**, *139*, 688–695. [CrossRef]

27. Jing, H.; Wang, X.; Liu, Y.; Wang, A. Preparation of Magnetic Nanocomposites of Solid Acid Catalysts and Their Applicability in Esterification. *Chin. J. Catal.* **2015**, *36*, 244–251. [CrossRef]

28. Jain, A.; Balasubramanian, R.; Srinivasan, M.P. Hydrothermal Conversion of Biomass Waste to Activated Carbon with High Porosity: A Review. *Chem. Eng. J.* **2016**, *283*, 789–805. [CrossRef]

29. Chellappan, S.; Aparna, K.; Chingakham, C.; Sajith, V.; Nair, V. Microwave Assisted Biodiesel Production Using a Novel BrØnsted Acid Catalyst Based on Nanomagnetic Biocomposite. *Fuel* **2019**, *246*, 268–276. [CrossRef]

30. Eterigho, E.J.; Alueshima, B.M.; Ejejigbe, S.E. Optimization of Process Parameters for the Synthesis of Locally Sourced Alumina-Supported Eggshell Catalyst. *Lect. Notes Eng. Comput. Sci.* **2018**, *2238*, 523–527.

31. Hussain, Z.; Kumar, R. Synthesis and Characterization of Novel Corncob-Based Solid Acid Catalyst for Biodiesel Production. *Ind. Eng. Chem. Res.* **2018**, *57*, 11645–11657. [CrossRef]

32. Liu, K.; Wang, R.; Yu, M. An Efficient, Recoverable Solid Base Catalyst of Magnetic Bamboo Charcoal: Preparation, Characterization, and Performance in Biodiesel Production. *Renew Energy* **2018**, *127*, 531–538. [CrossRef]

33. Abdedayem, A.; Guiza, M.; Ouederni, A. Copper Supported on Porous Activated Carbon Obtained by Wetness Impregnation: Effect of Preparation Conditions on the Ozonation Catalyst's Characteristics. *Comptes Rendus Chim.* **2015**, *18*, 100–109. [CrossRef]

34. Amadine, O.; Essamlali, Y.; Fihri, A.; Larzek, M.; Zahouily, M. Effect of Calcination Temperature on the Structure and Catalytic Performance of Copper-Ceria Mixed Oxide Catalysts in Phenol Hydroxylation. *RSC Adv.* **2017**, *7*, 12586–12597. [CrossRef]

35. Ding, Y.; Zhao, C.; Li, Y.; Ma, Z.; Lv, X. Effect of Calcination Temperature on the Structure and Catalytic Performance of the Cu-Mcm-41 Catalysts for the Synthesis of Dimethyl Carbonate. *Quim. Nova* **2018**, *41*, 1156–1161. [CrossRef]

36. Lu, J.; Zhao, Z.; Xu, C.; Duan, A.; Zhang, P. Effects of Calcination Temperature on the Acidity and Catalytic Performances of HZSM-5 Zeolite Catalysts for the Catalytic Cracking of n-Butane. *J. Nat. Gas Chem.* **2005**, *14*, 213–220. [CrossRef]

37. Zainol, M.M.; Amin, N.A.S.; Asmadi, M. Synthesis and Characterization of Porous Microspherical Ionic Liquid Carbon Cryogel Catalyst for Ethyl Levulinate Production. *Diam. Relat. Mater.* **2019**, *95*, 154–165. [CrossRef]

38. Zainol, M.M.; Amin, N.A.S.; Asmadi, M. Effects of Thermal Treatment on Carbon Cryogel Preparation for Catalytic Esterification of Levulinic Acid to Ethyl Levulinate. *Fuel Process. Technol.* **2017**, *167*, 431–441. [CrossRef]

39. Singh, S.; Kumar, R.; Setiabudi, H.D.; Nanda, S.; Vo, D.V.N. Advanced Synthesis Strategies of Mesoporous SBA-15 Supported Catalysts for Catalytic Reforming Applications: A State-of-the-Art Review. *Appl. Catal. A Gen.* **2018**, *559*, 57–74. [CrossRef]

40. He, B.; Fu, X.; Lian, X.; Jiang, S.; Xu, P.; Deng, X.; He, C.; Chen, C. Catalytic Deacidification of Vacuum Gas Oil by Zno/Al2o3 and Its Modification with Fe_2O_3. *Catalysts* **2019**, *9*, 499. [CrossRef]

41. Rosli, N.S.; Harun, S.; Jahim, J.M.; Othaman, R. Chemical and Physical Characterization of Oil Palm Empty Fruit Bunch. *Malays. J. Anal. Sci.* **2017**, *21*, 188–196. [CrossRef]

42. Agapay, R.C.; Liu, H.C.; Ju, Y.H.; Go, A.W.; Angkawijaya, A.E.; Nguyen, P.L.T.; Truong, C.T.; Quijote, K.L. Synthesis and Initial Evaluation of Solid Acid Catalyst Derived from Spent Coffee Grounds for the Esterification of Oleic Acid and Methanol. *Waste Biomass Valorization* **2021**, *12*, 4387–4397. [CrossRef]

43. Bureros, G.M.A.; Tanjay, A.A.; Cuizon, D.E.S.; Go, A.W.; Cabatingan, L.K.; Agapay, R.C.; Ju, Y.H. Cacao Shell-Derived Solid Acid Catalyst for Esterification of Oleic Acid with Methanol. *Renew Energy* **2019**, *138*, 489–501. [CrossRef]

44. Jenie, S.N.A.; Kristiani, A.; Sudiyarmanto; Khaerudini, D.S.; Takeishi, K. Sulfonated Magnetic Nanobiochar as Heterogeneous Acid Catalyst for Esterification Reaction. *J. Environ. Chem. Eng.* **2020**, *8*, 103912. [CrossRef]

45. Zhang, B.; Gao, M.; Geng, J.; Cheng, Y.; Wang, X.; Wu, C.; Wang, Q.; Liu, S.; Cheung, S.M. Catalytic Performance and Deactivation Mechanism of a One-Step Sulfonated Carbon-Based Solid-Acid Catalyst in an Esterification Reaction. *Renew Energy* **2021**, *164*, 824–832. [CrossRef]

46. Huang, M.; Luo, J.; Fang, Z.; Li, H. Biodiesel Production Catalyzed by Highly Acidic Carbonaceous Catalysts Synthesized via Carbonizing Lignin in Sub- and Super-Critical Ethanol. *Appl. Catal. B* **2016**, *190*, 103–114. [CrossRef]
47. Rechnia-Gorący, P.; Malaika, A.; Kozłowski, M. Acidic Activated Carbons as Catalysts of Biodiesel Formation. *Diam. Relat. Mater.* **2018**, *87*, 124–133. [CrossRef]